Supporting information for

Diniobium Inverted Sandwich Complexes with μ-η^6:η^6-arene Ligands: Synthesis, Kinetics of Formation, and Electronic Structure

Thomas L. Gianetti,[1] Grégory Nocton,[1,2] Stefan G. Minasian,[3,4] Neil C. Tomson,[1] A. L. David Kilcoyne,[5] Stosh A. Kozimor,[4] David K. Shuh,[3] Tolek Tyliszczak,[5] Robert G. Bergman[1]* and John Arnold.[1]*

[1]*Department of Chemistry, University of California, Berkeley, California 94720*
[2]*Laboratoire Hétéroéléments et Coordination, UMR CNRS 7653, Ecole Polytechnique, 91128 Palaiseau, France*
[3]*Chemical Sciences Division and Advanced Light Source, Lawrence Berkeley National Laboratory, Berkeley, CA 94720*
[4]*Inorganic, Isotope and Actinide Chemistry, Los Alamos National Laboratory, Los Alamos, NM 87545*
[5]*Advanced Light Source, Lawrence Berkeley National Laboratory, Berkeley, CA 94720*

A. Kinetic analysis of the formation of complex 7a

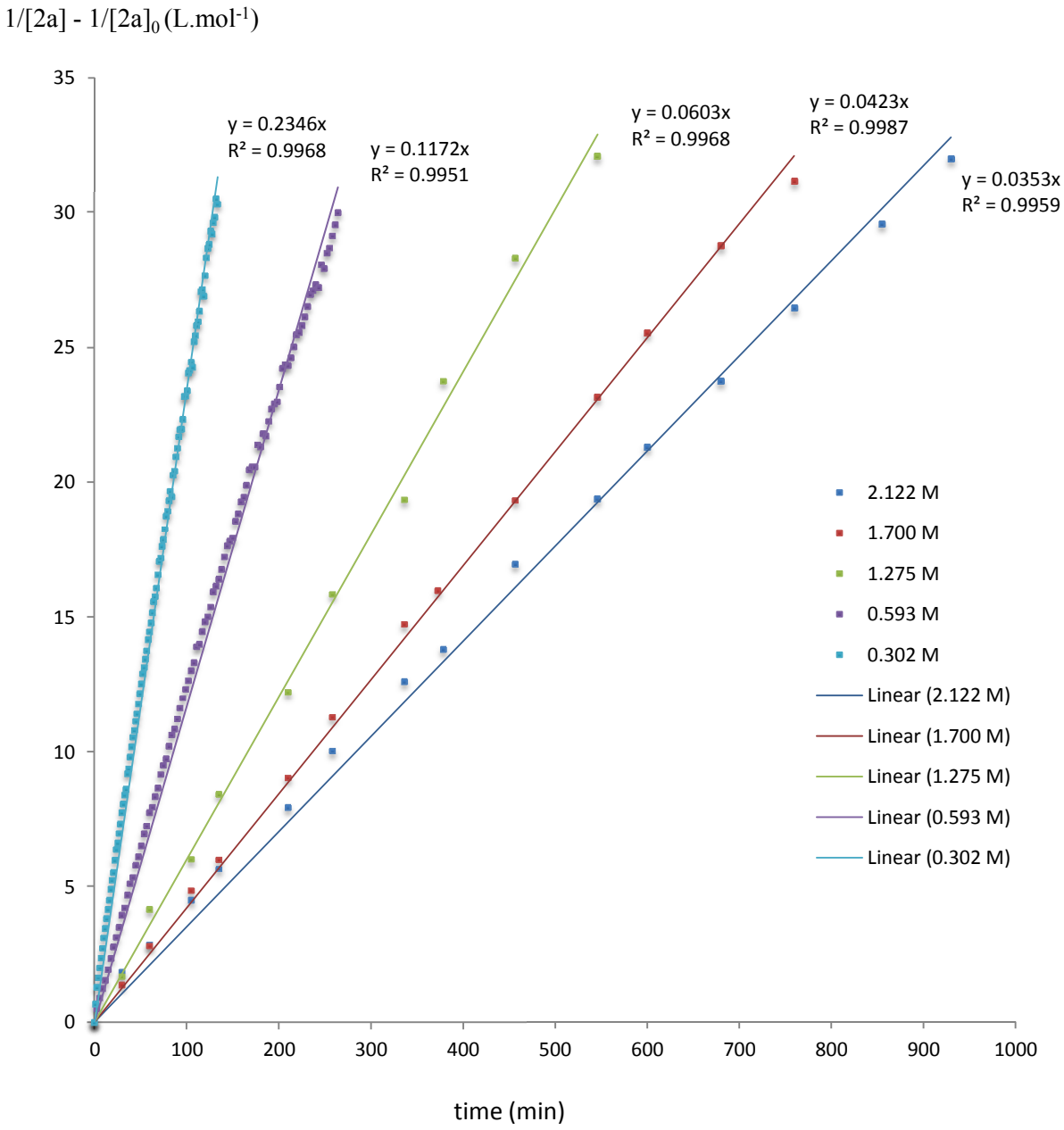

Figure S. 1 Second order fit of the conversion of complex 2a into **7a** at different concentrations of benzene [0. 30 – 2.12] M.

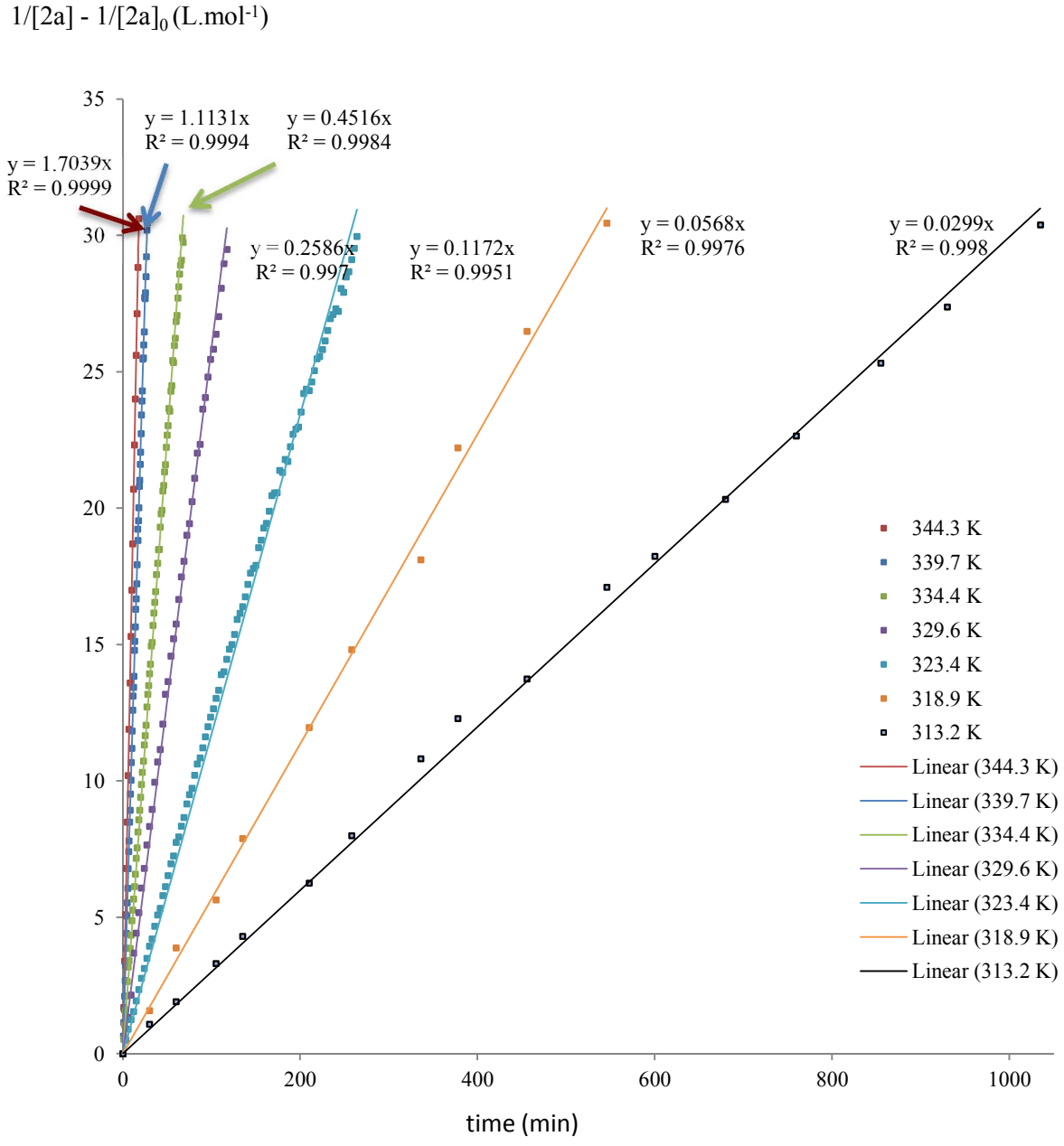

Figure S. 2 Second order fit of the conversion of complex **2a** into **7a** at different temperatures [313 – 344] K.

B. ^{1}H NMR spectroscopy analysis of complexes 7a-b and 9

B.1 NMR spectra of complex 7a at 233 K

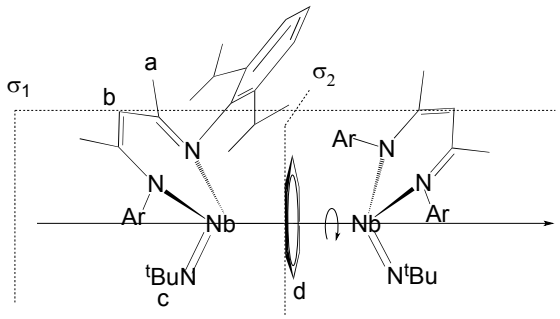

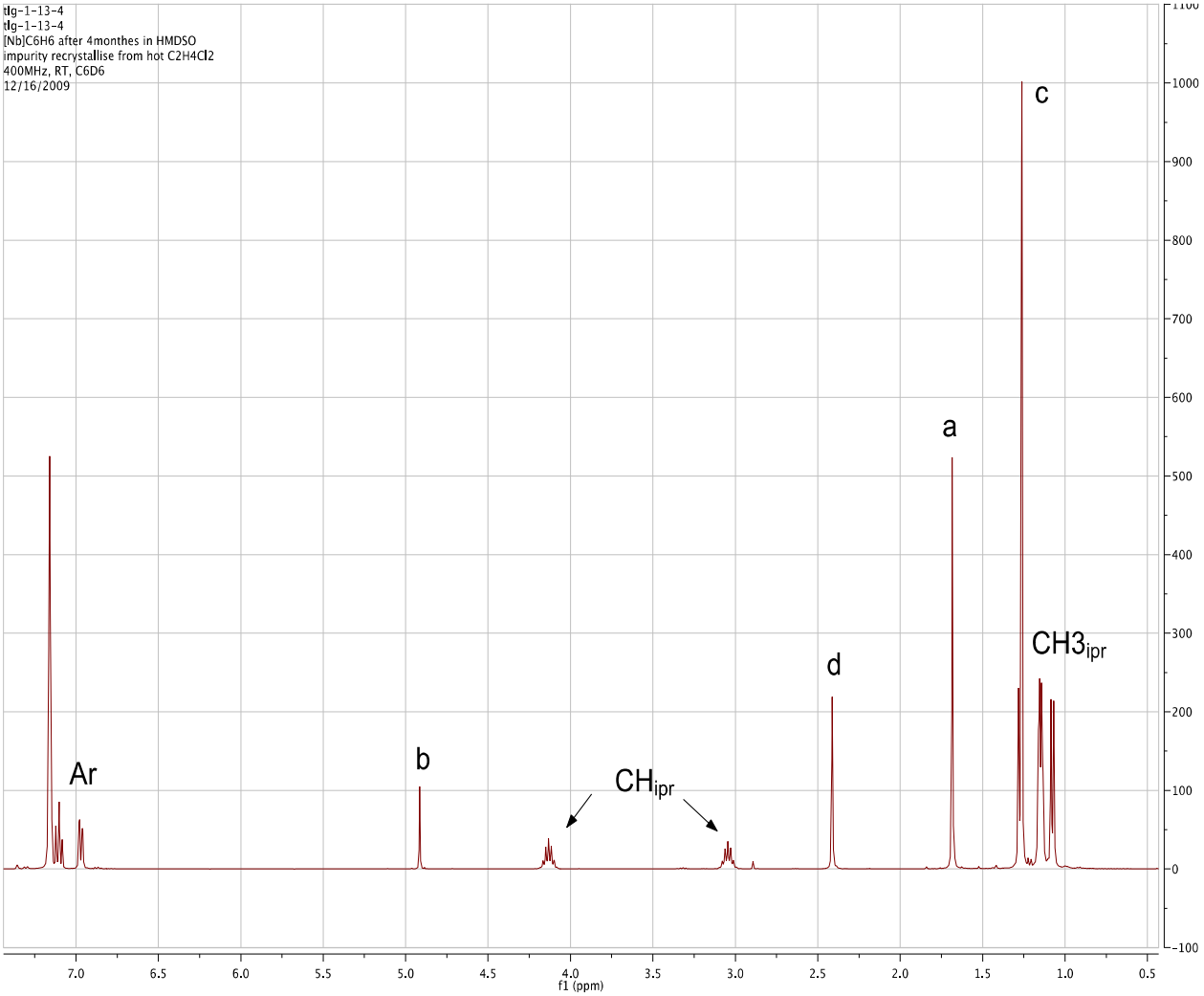

Figure S. 3 ^{1}H NMR spectrum of complex **7a** showing the high symmetry in solution due to the dynamic motion.

B.2 Variable temperature [213 K - 283 K] of complex 7b

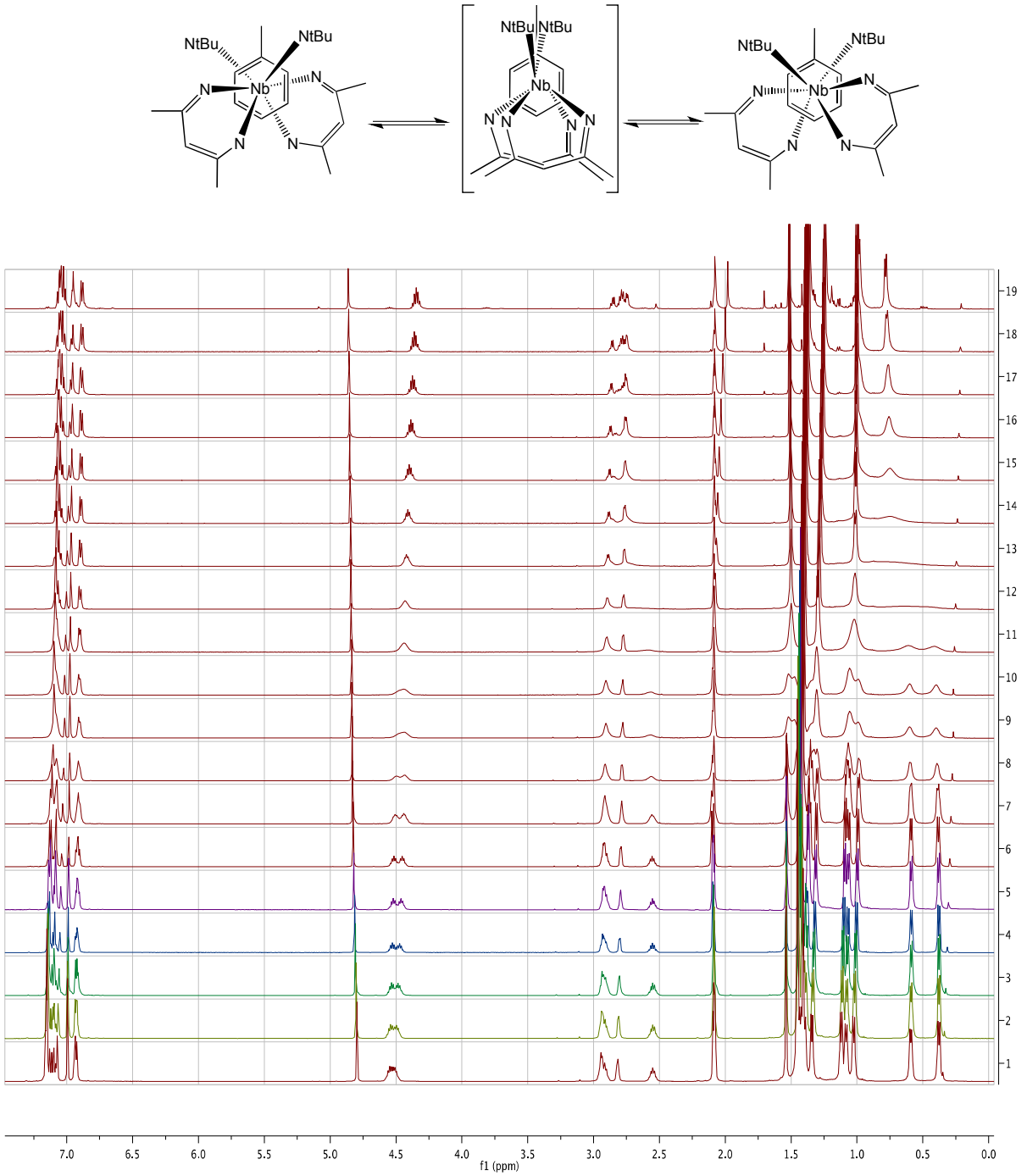

Figure S. 4 Variable temperature spectra from 213 K to 383 K of complex **7b**.

B.3 Variable temperature ^{1}H NMR [295 K - 230 K] of complex 9

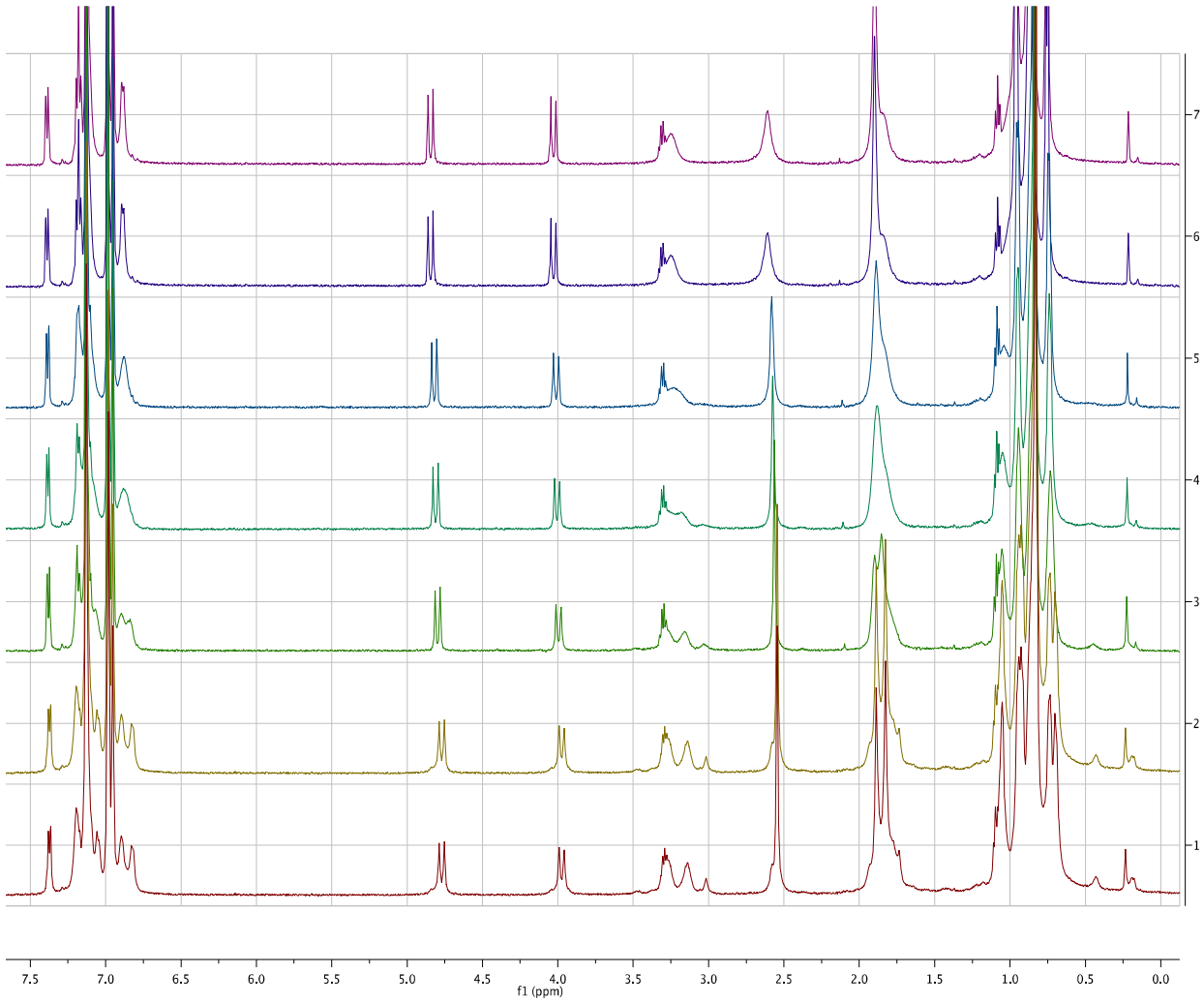

Figure S. 5 Variable temperature spectra from 295 K to 330 K of complex **9**.

B.4. Selective Inversion Recovery experiment

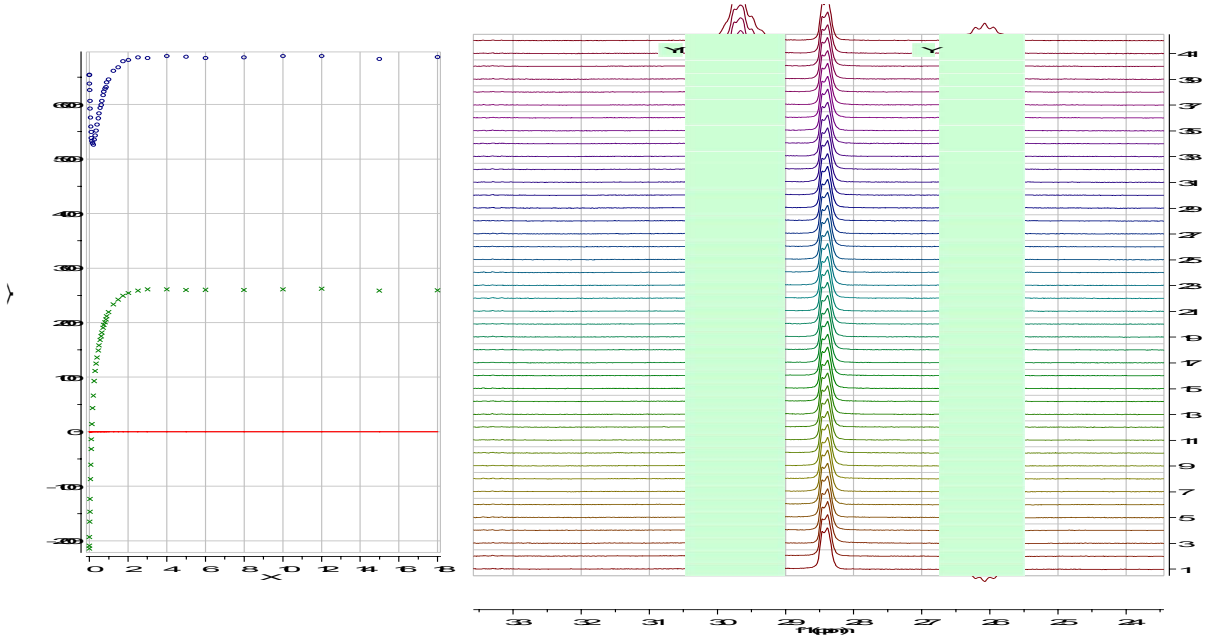

Figure S. 6 ^{1}H NMR spectra of complex **7b** at different mixing time from the SIR experiment at T = 253 K (right). Observed integral of the exchange resonance (top left) and of the saturated resonance (bottom left) from the SIR experiment at T = 253 K.

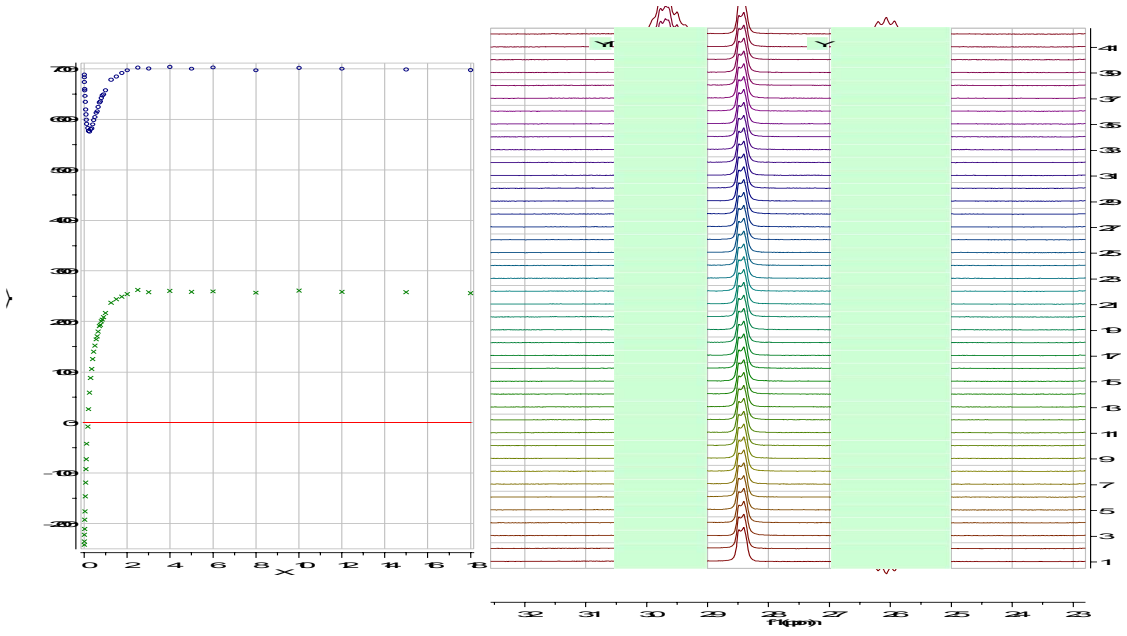

Figure S. 7 ^{1}H NMR spectra of complex **7b** at different mixing time from the SIR experiment at T = 263 K (right). Observed integral of the exchange resonance (top left) and of the saturated resonance (bottom left) from the SIR experiment at T = 263 K.

C. Representative procedure for X-ray crystallography

Table S. 1 Crystallographic parameters.

Compound	**2a**	**7a•$C_4H_{10}O$**	**7b•C_7H_8**	**8**	**9•$PhCF_3$**
Formula	$C_{39}H_{56}N_3Nb$	$C_{76}H_{116}N_6Nb_2O$	$C_{80}H_{116}N_6Nb_2$	$C_{96}H_{107}B_1F_{20}N_6Nb_2$	$C_{127}H_{124}B_2F_{43}N_6Nb_2$
Formula weight	659.78	1313.59	1347.61	1921.51	2742.64
Space Group	$P2_12_12_1$	$Pna2_1$	$Pna2_1$	P_{-1}	P_{-1}
a (Å)	9.9013(5)	21.775(4)	23.114(5)	14.834(5)	15.2951(10)
b (Å)	18.7383(11)	25.726(4)	17.957(4)	17.750(5)	19.8041(13)
c (Å)	18.9322(10)	12.645(2)	17.525(4)	17.811(5)	21.4734(15)
α (°)	90	90	90	82.109(5)	86.047(3)
β (°)	90	90	90	75.003(5)	73.864(4)
γ (°)	90	90	90	86.878(5)	74.382(3)
V (Å^3)	3512.6(3)	7083(2)	7274(3)	4486(2)	6017.4(7)
Z	4	4	4	2	2
ρ_{calcd} (g/cm^3)	1.248	1.234	1.231	1.422	1.514
F_{000}	1408	2816	2880	1984	2792
μ (mm^{-1})	0.373	0.370	0.361	0.347	0.310
T_{min}/T_{max}	0.9637/0.9852	0.9363/0.9639	0.8993/0.9892	0.9030 /0.9795	0.9265/0.9726
No. rflns measured	19888	111211	142569	82723	95984
No. indep. rflns	6335	12991	13354	16401	21919
R_{int}	0.0758	0.0322	0.0827	0.0312	0.0419
No. obs. ($I > 2.00\sigma(I)$)	6335	13169	13354	16401	21920
No. variables	425	807	822	1184	1627
R_1, wR_2	0.0473,0.0822	0.0205, 0.0500	0.0345, 0.0681	0.0304, 0.0659	0.03630, 0.0830
R_1 (all data)	0.0811	0.0223	0.0467	0.0425	0.0505
GoF	0.982	1.060	1.042	1.012	1.035
Res. peak/hole	0.365/-0.553	0.583/-0.122	0.800/-0.397	0.337/ -0.534	1.889/-0.847

($e^-/Å^3$)

C.1 ORTEP views for Complexes 2a, 7a-b, 8 and 9

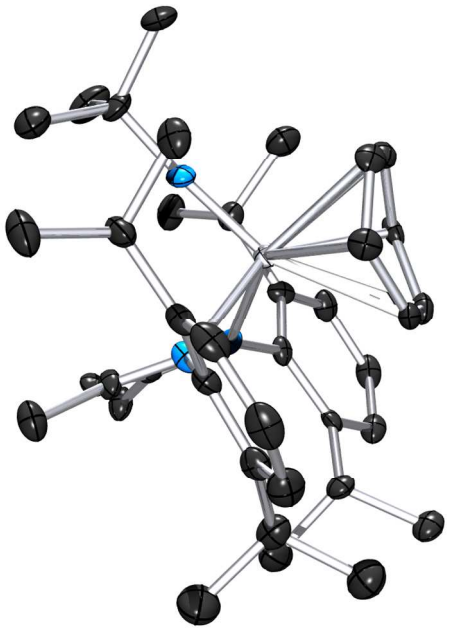

Figure S. 8 Ortep view of the full structure of complex **2a**.

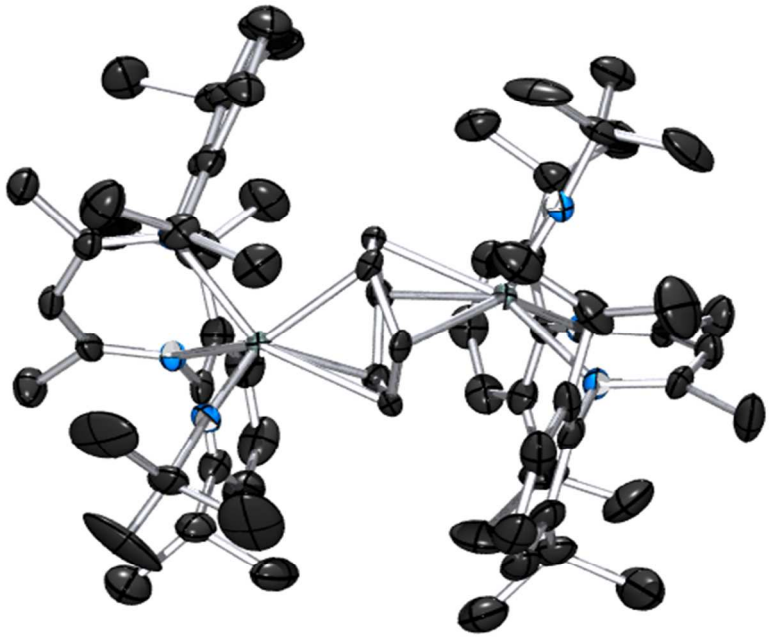

Figure S. 9 Ortep view of the full structure of complex **7a**.

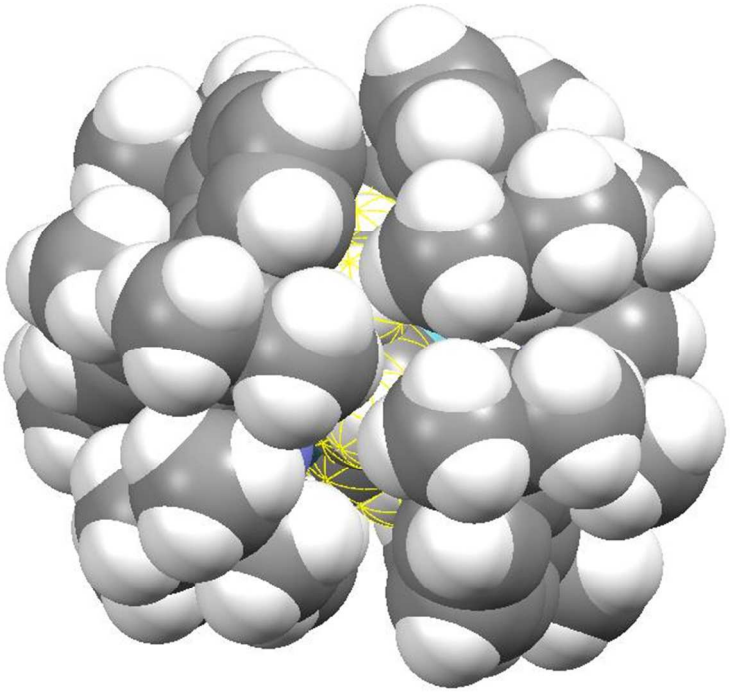

Figure S. 10 Spacefill view of **7a**. The benzene moiety is highlighted in yellow.

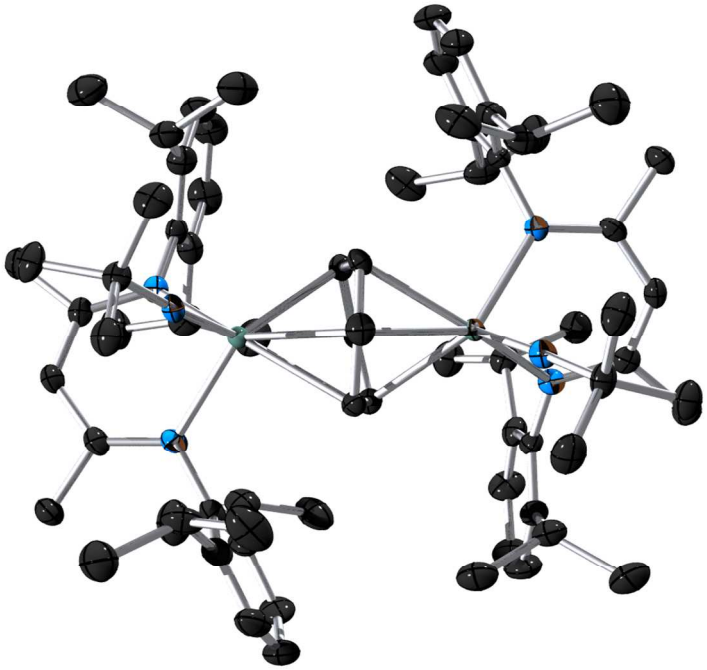

Figure S. 11 Ortep view of the full structure of complex **7b**.

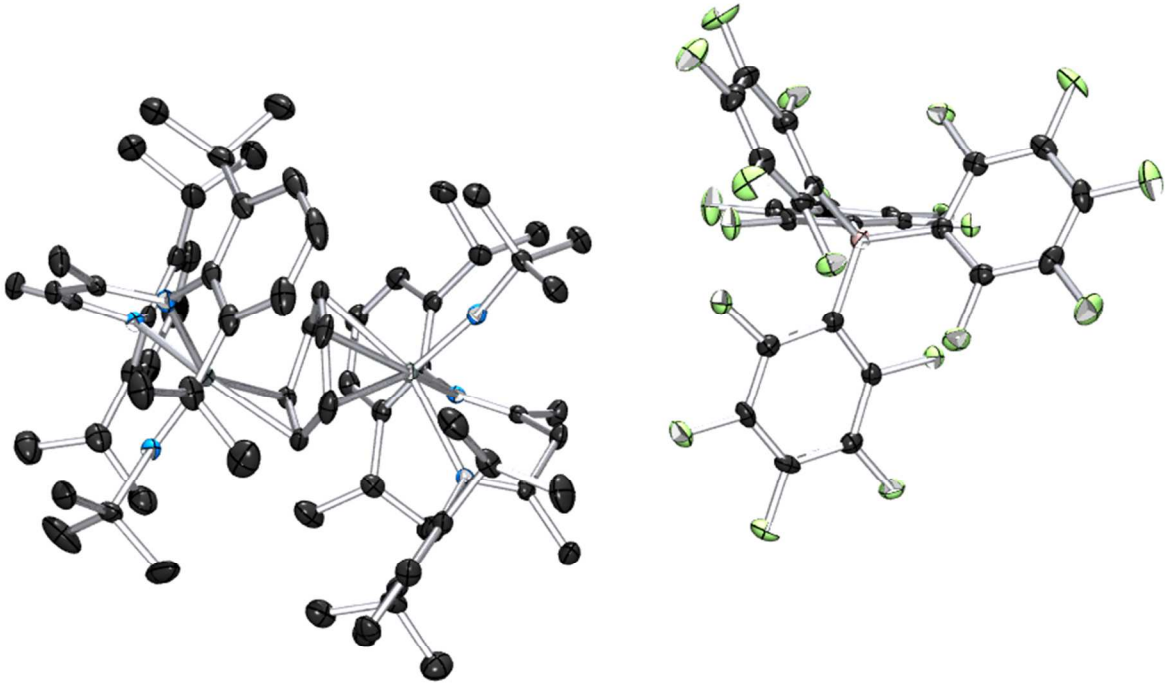

Figure S. 12 Ortep view of the full structure of complex **8**.

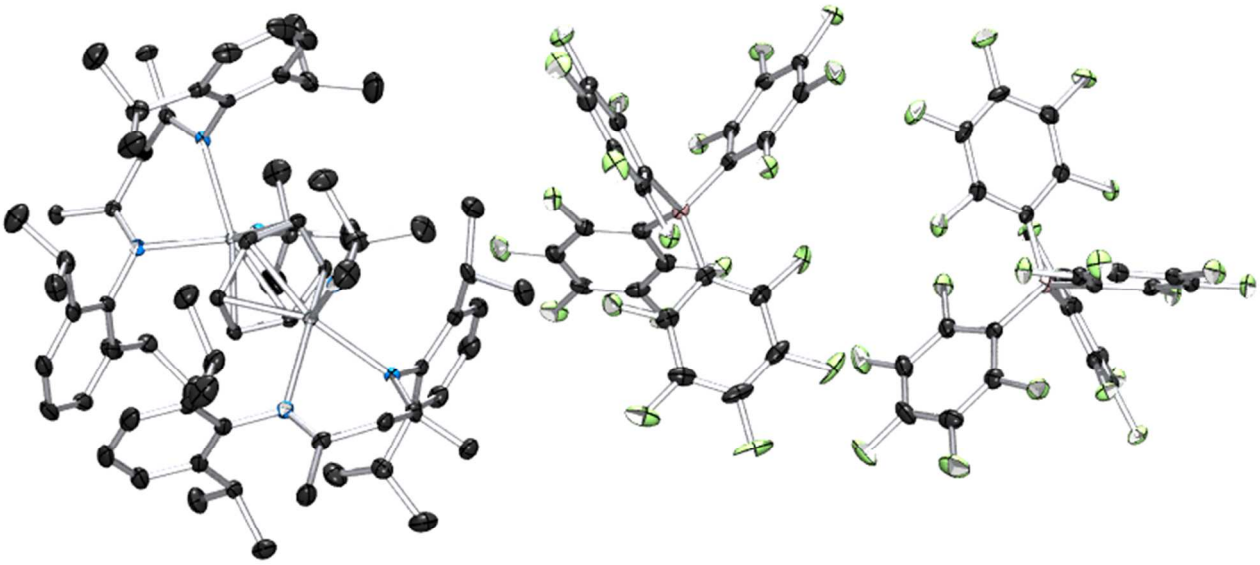

Figure S. 13 Ortep view of the full structure complex **9**.

C.2 Bond distances of (BDI)Nb(N^{t}Bu) moiety in Complexes 2a, 7a-b, 8 and 9

Table S. 2 Bond distances (in Å) of (BDI)Nb(N^{t}Bu) moiety for complexes **1**, **3, 4**, **5**, **7a-b**, **8**, **9** and **10**.

	Nb=N^{t}Bu	Nb-N_1 (BDI)	Nb-N_2 (BDI)	N_1-C□	N_2-C□
1: (BDI)Nb(N^{t}Bu)$(Me)_2$ [a]	1.7773 (13)	2.3578 (13)	2.1354 (13)	1.323 (2)	1.3557 (19)
2a: (BDI)Nb(N^{t}Bu)(C_6H_6)	1.775(6)	2.246(6)	2.246(6)	1.329(5)	1.337(5)
3: (BDI)Nb(N^{t}Bu)$(CO)_2$ [a]	1.792(3)	2.223(3)	2.191(3)	1.346(5)	1.343(5)
4: (BDI)Nb(N^{t}Bu)$(CNXyl)_3$ [a]	1.789(2)	2.286(2)	2.268(2)	1.332(4)	1.338(3)
5: [(BDI)Nb(N^{t}Bu)(μ-O)]$_2$ [b]	1.764(3)	2.218(3)	2.227(3)	1.345(5)	1.337(4)
7a: [(BDI)Nb(N^{t}Bu)]$_2$(C_6H_6) [b,c]	1.7770(15) 1.7815(15)	2.2136(17) 2.2266(15)	2.2764(16) 2.2787(16)	1.332(2) 1.342(2)	1.329(2) 1.335(2)
7b: [(BDI)Nb(N^{t}Bu)]$_2$(C_7H_8) [b,c]	1.776(3) 1.782(3)	2.249(3) 2.241(3)	2.271(3) 2.271(3)	1.339(4) 1.334(5)	1.332(4) 1.332(4)
8: [(BDI)Nb(N^{t}Bu)]$_2$(C_6H_6) [b,c,d]	1.7718(19) 1.7860(18)	2.2055(18) 2.3109(17)	2.2209(18) 2.3236(18)	1.337(3) 1.290(3)	1.335(3) 1.284(3)
9: [(BDI)Nb(N^{t}Bu)]$_2$(C_6H_6) [b,c]	1.774(2) 1.7819(19)	2.289(2) 2.2983(19)	2.3226(19) 2.3287(19)	1.290(3) 1.294(3)	1.293(3) 1.289(3)
10: (BDI)Nb(N^{t}Bu)(py)$(Cl)_2$ [a]	1.765(2)	2.420(2)	2.100(2)	1.317(3)	1.369(3)

a: N_1 is trans to the imido moiety. b: The imido/BDI are on the fac- of a pseudo octahedron, c: values in the same column are related by the C_2 axis. d: the first row correspond to the non-protonated moiety.

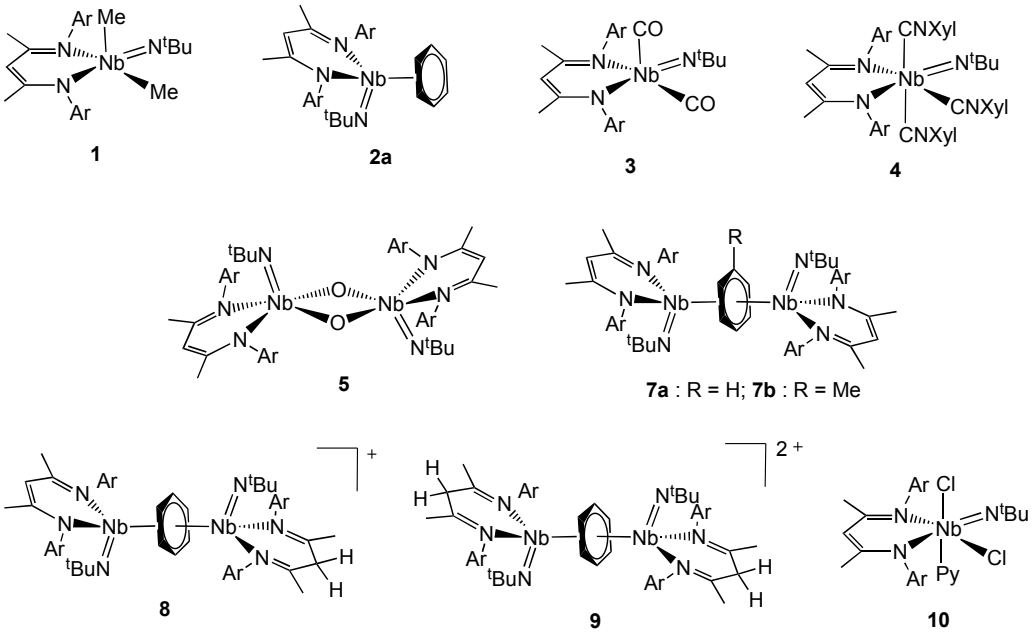

Figure S. 14 Chemdraw representations of complexes **1**, **3**, **4**, **5**, **7a-b**, **8**, **9** and **10**. Complexes **1**, **3, 4** and **10** have the imido group in the basal position leading to disymmetric Nb-BDI bond distance (top). Complex **5**, **2a, 7a-b**, **8** and **9** have the imido/BDI groups on the facial positions of a pseudo octahedron, leading to quasi-symmetric Nb-BDI bond distances (bottom).

C.3 Distorsion of the arene ring in Complexes 7a-b, 8 and 9

The distorsion of the arene ring was estimated by observing the deviation from each carbon and the mean plane formed by the full arene moiety (left part of figure S.17 to S.20) as well as the three dihedral angles formed between the 6 planes of the arene moiety (right part of figure S.17 to S.20)

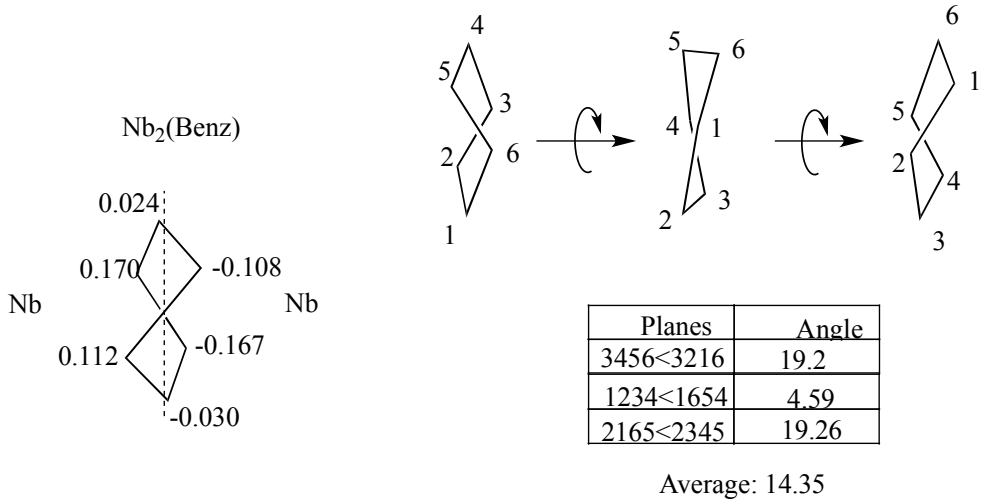

Planes	Angle
3456<3216	19.2
1234<1654	4.59
2165<2345	19.26

Average: 14.35

Figure S. 15 Distortion of the benzene ring in complex **7a**

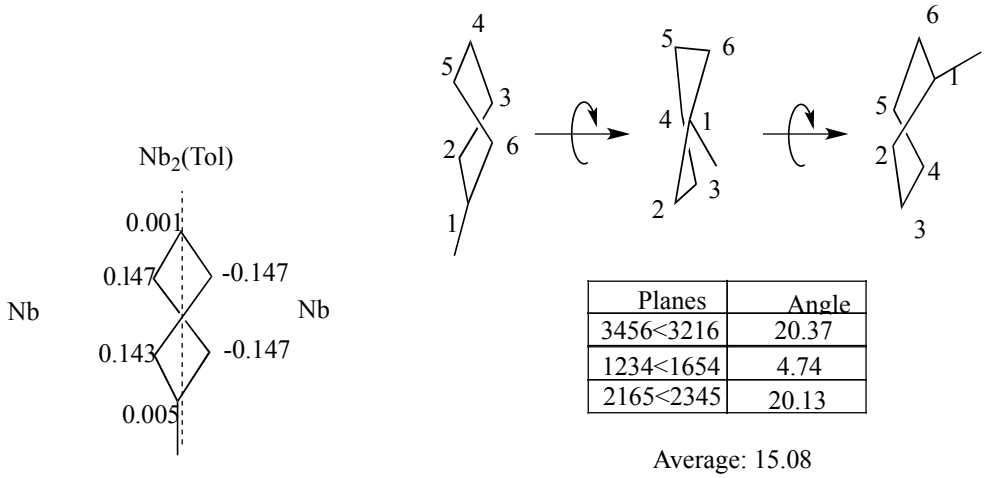

Planes	Angle
3456<3216	20.37
1234<1654	4.74
2165<2345	20.13

Average: 15.08

Figure S. 16 Distortion of the toluene ring in complex **7b**

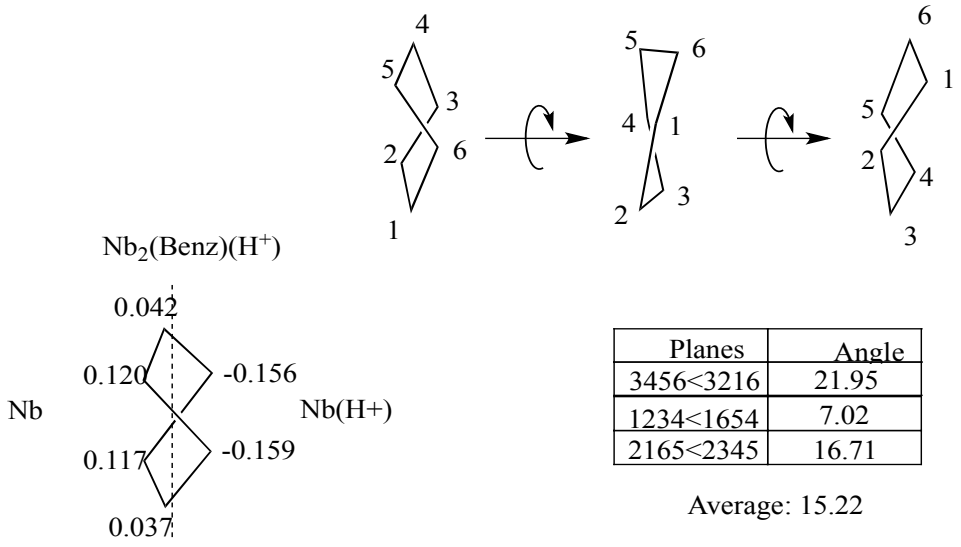

Planes	Angle
3456<3216	21.95
1234<1654	7.02
2165<2345	16.71

Average: 15.22

Figure S. 17 Distortion of the benzene ring in complex **8**

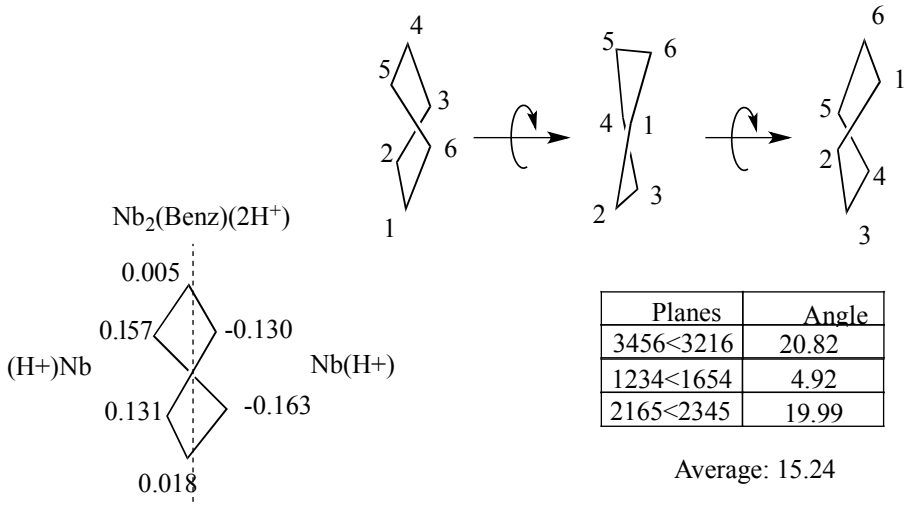

Planes	Angle
3456<3216	20.82
1234<1654	4.92
2165<2345	19.99

Average: 15.24

Figure S. 18 Distortion of the benzene ring in complex **9**